World Electric Vehicle Journal

MDPI

Article

Dual-Fuzzy Regenerative Braking Control Strategy Based on Braking Intention Recognition

Yaning Qin, Zhu'an Zheng * and Jialing Chen

School of Automotive Engineering, Yancheng Institute of Technology, Yancheng 224051, China; qinyaning@ycit.edu.cn (Y.Q.); 18262883652@163.com (J.C.)
* Correspondence: zza@ycit.edu.cn

Abstract: Regenerative braking energy recovery is of critical importance for electric vehicles due to their range limitations. To further enhance regenerative braking energy recovery, a dual-fuzzy regenerative braking control strategy based on braking intention recognition is proposed. Firstly, the distribution strategy for braking force is devised by considering classical curves like ideal braking force allocation and ECE regulations; secondly, taking the brake pedal opening and its opening change rate as inputs, the braking intention recognition fuzzy controller is designed for outputting braking strength. Based on the recognized braking strength, and considering the battery charging state and the speed of the vehicle as inputs, a regenerative braking duty ratio fuzzy controller is developed for regenerative braking force regulation to improve energy recovery. Furthermore, a control experiment is established to evaluate and compare the four models and their respective nine braking modes, aiming to define the dual fuzzy logic controller model. Ultimately, simulation validation is conducted using Matlab/Simulink R2019b and CRUISE 2019. The results show that the strategy in this paper has higher energy savings compared to the single fuzzy control and parallel control methods, with energy recovery improved by 26.26 kJ and 96.13 kJ under a single New European Driving Cycle (NEDC), respectively.

Keywords: braking intention recognition; regenerative braking; fuzzy algorithm; energy recovery; braking force distribution

Citation: Qin, Y.; Zheng, Z.; Chen, J. Dual-Fuzzy Regenerative Braking Control Strategy Based on Braking Intention Recognition. *World Electr. Veh. J.* **2024**, *15*, 524. https://doi.org/10.3390/wevj15110524

Academic Editor: Joeri Van Mierlo

Received: 27 October 2024
Revised: 11 November 2024
Accepted: 12 November 2024
Published: 14 November 2024

1. Introduction

In the current era, environmental pollution has emerged as a pressing global issue, with motor vehicle exhaust emissions serving as a prominent source of air contamination. To address these environmental challenges, nations have actively advocated for the advancement of clean energy vehicles [1]. Among these alternatives, electric vehicles have progressively risen in popularity as the predominant choice, attributed to their benefits, such as emission reduction and minimal noise output. Nevertheless, the expanding acceptance of electric vehicles has brought to light the issue of limited range, posing a significant obstacle to their ongoing development [2]. Regenerative braking in electric vehicles utilizes the drive motor to convert a portion of kinetic energy into electrical energy during braking, thereby enhancing energy efficiency and extending the vehicle's range [3,4]. This technique stands out as a potent method for range extension, underscoring its profound importance in furthering the efficiency of electric vehicles.

Electric vehicles employ a combined braking system that integrates regenerative braking with traditional mechanical braking components [5], whose overall control difficulty is significantly higher than that of the traditional mechanical braking system. Therefore, to guarantee both safety during braking maneuvers and the recuperation of energy, scholars have carried out a lot of research on composite brake control.

In the area of driver braking intention recognition: Due to the driver's subjective factors, it is impossible to measure the braking intention directly, and it can only be accurately

recognized by extracting feature parameters. A wide range of scholars have conducted research from different perspectives, such as braking feature parameter extraction and braking intention recognition control algorithms [6]. For braking characteristic parameter selection, Wen Jianping et al. [7] obtained a multidimensional feature vector of the braking signal by modal decomposition and feature extraction of the brake pedal signal; they then combined the sparrow search algorithm with a probabilistic neural network to establish a model for recognizing braking intentions; and finally, they experimentally verified that the model has a high recognition accuracy. Luis G. Hernandez et al. [8] proposed a method for recognizing emergency braking intention based on the driver's electrical brain signals. By collecting vehicle data and brain signals and performing emergency braking in different situations, the findings indicated that the method achieved an 80% accuracy rate in classification. Li Min et al. [9] used the driver's EEG signal as an input parameter for recognizing the driver's behavior and intention. Based on the experimental findings, it is evident that the model demonstrates a notable level of recognition accuracy. Stefan Haufe et al. [10] validated the feasibility of electrophysiology-based emergency braking intention detection through real-vehicle driving tests. On this basis, Hermes J. Mora et al. [11] proposed a simple and accurate emergency braking intention detection method by combining the driver's EEG signals with neural networks, which solved the problem of long EEG signal processing time. Considering the driver's fatigue and stress, Oscar Martinez Mozos et al. [12] used support vector machines and convolutional neural networks to classify the EEG signals, with a classification accuracy of more than 80%. For braking intention recognition control algorithms, Tang Jinhua et al. [13] constructed a braking intention recognition model by fuzzifying multiple sets of braking test data, and trained and tested the model. Finally, the method was verified offline to have a high braking intention recognition accuracy. Jia Qiyang et al. [14] designed a braking intention recognition controller based on a large amount of driving data and fuzzy control principles. The braking intention recognition model's accuracy underwent validation through collaborative simulation. Yang Wei et al. [15] introduced a braking intention recognition model for leading vehicles. This model integrates the BP neural network and Hidden Markov Model, tailored for automatic emergency braking systems. The model can dynamically change the critical braking distance under different driving conditions. Wang Shu et al. [16] proposed a braking intention recognition method based on a long- and short-term memory network, using a support vector machine-recursive feature elimination algorithm for feature parameter selection, and real-vehicle experiments proved that the accuracy of the recognition model can reach more than 95%.

In terms of braking force distribution: Jiang et al. [17] proposed a distribution strategy based on an optimal distribution algorithm and improved the braking energy recovery efficiency by more than 51.9% compared to the control strategy of the ADVISOR software. Liu et al. [18] introduced a control scheme for the adaptive distribution of braking force, with the maximum regenerative braking torque as the inflection point and the synchronous attachment coefficient as the expected point. The findings indicated that the strategy can not only adapt to driving conditions but also improve the braking energy recovery efficiency. Pei et al. [19] introduced a control strategy for coordinated electric-hydraulic braking in electric vehicles. Utilizing a genetic algorithm, the team optimized distribution coefficients for varied braking scenarios. The results show that the strategy has better energy regeneration performance and braking stability than the ideal braking force allocation.

In terms of energy recovery: He et al. [20] proposed an energy recovery optimization strategy based on braking safety and efficient recovery, which both improved the energy recovery and shortened the braking distance. Zhang et al. [21] proposed a new predictive control method. Firstly, a prediction method was used to predict the vehicle speed and braking strength; secondly, a dynamic planning method was applied to optimize target torque and target pressure, and the outcomes indicate a notable enhancement in energy recovery efficiency. Zhang et al. [22] presented a regenerative braking control strategy that leverages collective intelligence. This strategy integrates an ant colony algorithm to

refine the iterative procedure of the particle swarm algorithm. The efficacy of the control method's stability was confirmed across diverse operational scenarios. Geng et al. [23] proposed a hierarchical braking energy recovery control strategy for hybrid vehicles, where the upper control aims to improve the front axle braking allocation percentage, and the lower control obtains the regenerative braking ratio coefficient. Finally, a model combining AMESim and Matlab/Simulink was built, and the results showed that the brake energy recovery rate was significantly improved.

In the above studies, scholars have used different methods to achieve the recognition of driver braking intention to some extent or to optimize the electric braking force using various algorithms to increase energy recovery. However, limited research has been conducted on the simultaneous optimization of recognizing driver braking intentions and coordinating composite braking forces, as well as the effect of fuzzy controller structure on the regenerative braking ratio. Therefore, in this paper, a dual fuzzy logic regenerative braking controller is designed by considering the braking intention of the driver of an electric vehicle, and the effect of various strategies on braking energy recovery in electric vehicles is also investigated.

2. Braking Force Distribution Strategy Design

How braking force is shared between the front and rear axles affects safety and energy recovery. A reasonable braking force distribution strategy can realize as much energy recovery as possible while prioritizing safety and stability during braking [24]. It is also key to preventing wheel locking.

2.1. Braking Dynamics Analysis

Before designing a regenerative braking strategy it is necessary to first analyze the dynamics of the front and rear axle wheels during braking. As depicted below in Figure 1, the illustration showcases the forces acting on the vehicle when braking on a flat roadway.

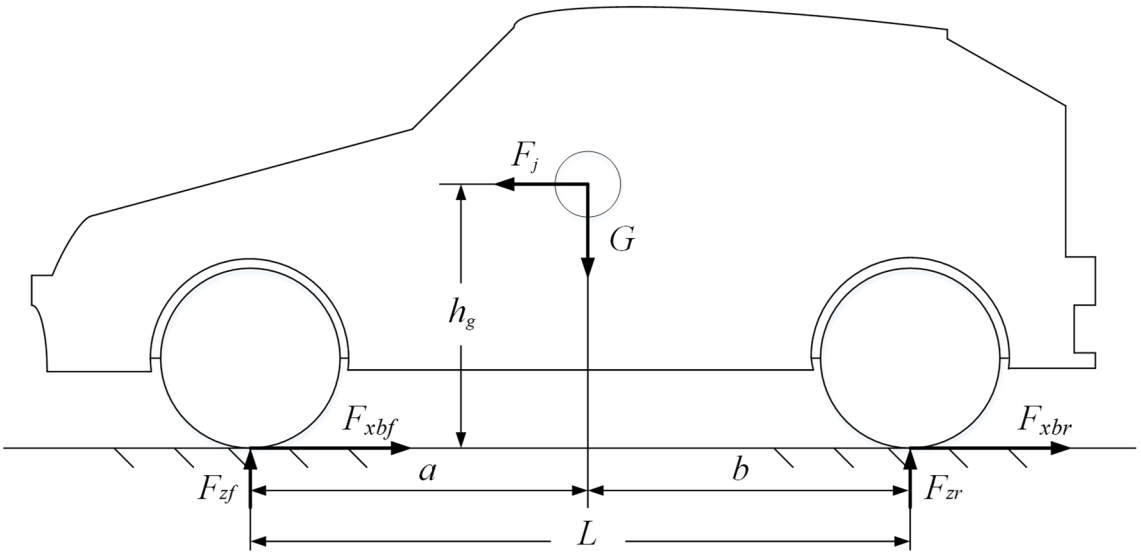

Figure 1. Vehicle braking force analysis.

In the figure, F_j is the inertial force (N).

The force situation at this point ignores the air resistance, rolling resistance, and the moment of inertia of the rotating mass during decelerating. According to the force analysis, the following moment balance equation can be obtained by taking moments on the front and rear axes:

$$\begin{cases} F_{zf}L = Gb + m\frac{du}{dt}h_g \\ F_{zr}L = Ga - m\frac{du}{dt}h_g \end{cases} \quad (1)$$

where F_{zf} and F_{zr} are the normal reaction force (N) exerted by the front and rear wheels on the ground; G is the car's gravitational force (N); L is the wheelbase (m); m is the car's mass (kg); a and b are the distances of the two axles from the center of gravity (m); du/dt is the deceleration of the car (m/s^2); and h_g is the height of the center of mass (m).

Let $du/dt = zg$ and z be the braking strength; then the ground's normal reaction force on both the front and rear wheels can be represented as:

$$\begin{cases} F_{zf} = \frac{G}{L}(b + zh_g) \\ F_{zr} = \frac{G}{L}(a - zh_g) \end{cases} \tag{2}$$

2.2. Braking Force Distribution Constraints

In order to take into account braking safety and energy recovery, the distribution of braking force for the front and rear axles should fall within the region bounded by the ideal braking force curve I, the ECE regulation line, and the f curve [25]. Assuming that F_{xb} is the total ground braking force (N), φ is the road surface adhesion coefficient, and F_{xbf} and F_{xbr} represent the ground braking forces (N) exerted by the front and rear axles, respectively. Subsequently, diverse conditions impose specific limitations on brake force distribution.

Ideal braking force distribution constraints, as shown in Equation (3):

$$F_{xbr} = \frac{1}{2}\left[\frac{G}{h_g}\sqrt{b^2 + \frac{4h_g L}{G}F_{xbf}} - \left(\frac{Gb}{h_g} + 2F_{xf}\right)\right] \tag{3}$$

The limitations on front and rear axle brake force distribution, as outlined in Equation (4) by the ECE regulations, are displayed:

$$\begin{cases} F_{xbf} = \frac{z+0.07}{0.85} \cdot \frac{G(b+Zh_g)}{L} \\ F_{xbr} = Gz - F_{xbf} \end{cases} \tag{4}$$

The requirements imposed on the front and rear axle braking force by the f-curve are presented in Equation (5):

$$F_{xbr} = \frac{L - \varphi h_g}{\varphi h_g}F_{xbf} - \frac{Gb}{h_g} \tag{5}$$

2.3. Braking Force Distribution Based on Limiting Boundary Conditions

This paper presents braking force distribution curves for the front and rear axle based on vehicle dynamics and braking force distribution constraints, divided into four segments, as shown in Figure 2.

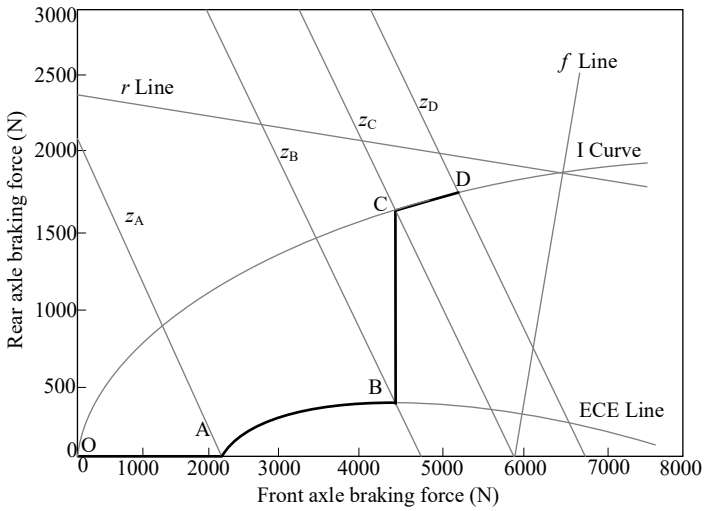

Figure 2. Braking force distribution scheme.

(1) OA section: pure motor brake

The braking demand in this section is small, requiring only motor brakes. Braking requirements for the front and rear axles:

$$\begin{cases} F_{xbf} = Gz \\ F_{xbr} = 0 \end{cases} \tag{6}$$

(2) AB section: pure motor brake

At this stage, with the increase in braking strength, the braking demand becomes larger, and motor braking alone cannot meet the requirements. At this time, both the motor brake and mechanical brake are engaged; the front and rear axle braking force is:

$$\begin{cases} F_{xbf} = \frac{z+0.07}{0.85} \times \frac{G\left(b+h_g z\right)}{L} \\ F_{xbr} = Gz - F_{xbf} \end{cases} \tag{7}$$

(3) BC section: pure motor brake

At this stage, the braking strength is greater, so the motor brake and mechanical brake work at the same time to meet the braking demand; the front and rear axle braking force is:

$$\begin{cases} F_{xbr} = \frac{G\left(zL-\varphi h_g z-\varphi b\right)}{L} \\ F_{xbf} = Gz - F_{xbr} \end{cases} \tag{8}$$

(4) CD section: pure motor brake

At this stage, the braking strength is too high, and the vehicle is subjected to emergency braking. The primary consideration is braking safety, and the work is carried out by mechanical braking alone, with front and rear axle braking forces:

$$\begin{cases} F_{xbr} = \frac{G\varphi\left(a-h_g z\right)}{L} \\ F_{xbf} = \frac{G\varphi\left(b+h_g z\right)}{L} \end{cases} \tag{9}$$

3. Dual Fuzzy Regenerative Braking Control Strategy

Utilizing the front and rear axle braking force distribution plan developed within defined constraints, a dual-fuzzy regenerative braking control strategy is formulated, incorporating driver braking intention recognition and energy recovery considerations. The braking intention recognition fuzzy controller is used to recognize the driver's braking intention, and the regenerative braking duty ratio fuzzy controller is used to distribute the electromechanical composite braking force.

3.1. Braking Intention Recognition

Brake intention recognition is a method of pattern recognition in computer technology, and its accurate recognition is of great significance in improving the accurate control of the braking system. In regenerative braking, brake intention recognition can improve the braking performance by recognizing the braking strength information.

Cluster analysis, neural networks, Markov models, and fuzzy logic systems are among the frequently employed techniques for recognizing brake intentions. Considering that cluster analysis needs to pre-process the braking characteristic parameters and that the selection of characteristic parameters has a large impact on the results, artificial neural networks have a large amount of computational workload and long processing times, and the application of Hidden Markov Models necessitates a substantial corpus of training data, which presents a challenge in accurately discerning conventional braking intentions. Fuzzy inference systems offer a compelling alternative, exhibiting superior flexibility, robust

anti-interference capabilities, and real-time control. This paper employs a fuzzy inference system to identify braking intentions.

3.2. Double Fuzzy Logic Controller Design

3.2.1. Feature Parameter Extraction

The accuracy of driver braking intention recognition depends on the selection of characteristic parameters. Commonly used recognition parameters are brake pedal opening, pedal change rate, brake pedal force, and brake line oil pressure. Considering that the pedal force is affected by many factors, which causes it to fluctuate and has a certain degree of randomness, the brake line oil pressure is generally used only as a redundant design scheme to improve the reliability of the brake system intent recognition; and driving habits impact the rate of change in brake pedal opening. Therefore, the brake pedal opening degree is selected as the characteristic parameter for brake intention recognition. Meanwhile, in order to identify the driver's braking urgency, the rate of change of brake pedal opening is introduced to identify the braking urgency.

When the driver performs a braking operation, the deceleration of the vehicle can be expressed as:

$$\frac{dv}{dt} = \frac{F_\mu}{m} \tag{10}$$

where dv/dt is the vehicle's braking deceleration (m/s^2) and F_μ is the vehicle's brake force (N).

In this paper, the braking strength is defined as the output of the braking intention recognition controller, as shown in the following equation:

$$zg = \frac{dv}{dt} \tag{11}$$

where z is the braking strength and g is the acceleration of gravity (m/s^2).

Figure 3 displays the configuration of the fuzzy controller for recognizing driver braking intentions.

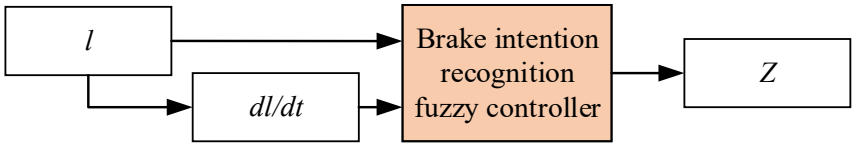

Figure 3. Braking intention recognition fuzzy controller structure.

The regenerative braking duty ratio is not only related to the recognized braking strength but also in relation to speed and battery State Of Charge (*SOC*). When speed is high, the regenerative braking percentage should be appropriately reduced in consideration of braking safety; when the battery *SOC* reaches a certain amount, regenerative braking should be reduced to prevent overcharging.

The structure of the regenerative braking duty ratio fuzzy controller is shown in Figure 4.

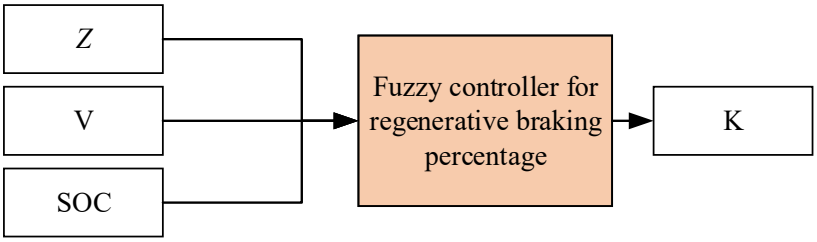

Figure 4. Regenerative braking duty ratio fuzzy controller structure.

3.2.2. Dual Fuzzy Logic Controller Structure

The structure of the fuzzy controller depends on the number of rules. Adding inputs can improve accuracy, but the fuzzy rules grow exponentially. In this paper, there are four inputs—brake pedal opening, brake pedal opening change rate, vehicle speed, and battery *SOC*. To enhance operational speed and minimize controller computations, a dual fuzzy controller has been devised, with its configuration depicted in Figure 5.

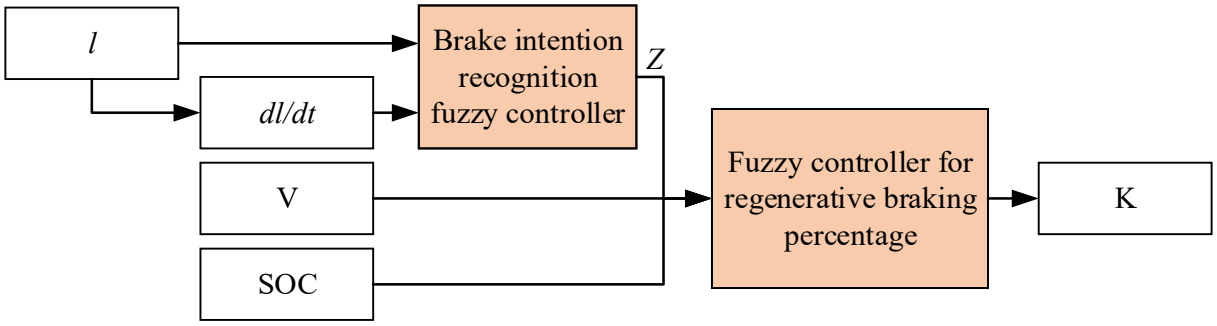

Figure 5. Dual fuzzy controller structure.

3.2.3. Fuzzy Rule Formulation and Affiliation Function Design

Based on the above feature parameter extraction, for the brake intention recognition fuzzy controller, the fuzzy domain of brake pedal opening l is defined as [0, 1], and the fuzzy subsets are {S (Small), M (Medium), B (Big)}; the fuzzy domain of the change rate of brake pedal opening dl/dt is defined as [−0.4, 1.6], and the fuzzy subsets are {L (Slow), M (Medium), F (Fast)}; the fuzzy domain of brake strength z is defined as [0, 1] with the fuzzy subsets {S (Small), M (Medium), B (Big)}.

For the brake intention recognition fuzzy controller, the fuzzy rules are formulated based on the fact that the greater the brake pedal opening and the greater the rate of change of the brake pedal opening, the more urgent the driver's braking needs. Based on this logical inference, the fuzzy rules for the braking intention recognition fuzzy controller can be obtained, as shown in Table 1.

Table 1. Fuzzy rules for the fuzzy controller for braking intention recognition.

dl/dt \ *l*	**S**	**M**	**B**
L	S	M	B
M	S	M	B
F	S	B	B

The surface map of the recognition effect of the fuzzy controller for braking intention recognition, obtained from the fuzzy rules formulated in Table 1, is shown in Figure 6.

Analysis of Figure 6 shows that the braking strength is mainly related to the brake pedal opening; the larger the brake pedal opening, the greater the required braking strength. When the brake pedal opening is subordinate to the intermediate subset, and the rate of change of the brake pedal opening is very fast, the identified demand braking strength is larger. The recognition results of the fuzzy controller for brake intention recognition are consistent with the driver's braking operation demands, which verifies the effectiveness of the fuzzy rules.

The affiliation functions of the input and output variables of the brake intention recognition fuzzy controller are shown in Figure 7.

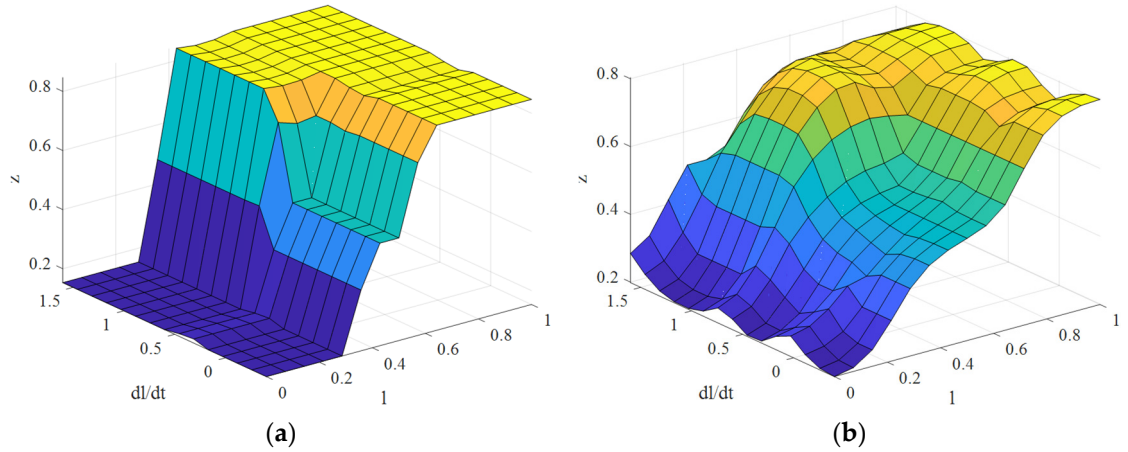

Figure 6. Variables relationship surface of the fuzzy controller for braking intention recognition. (**a**) T_T-type affiliation function; (**b**) G_S-type affiliation function.

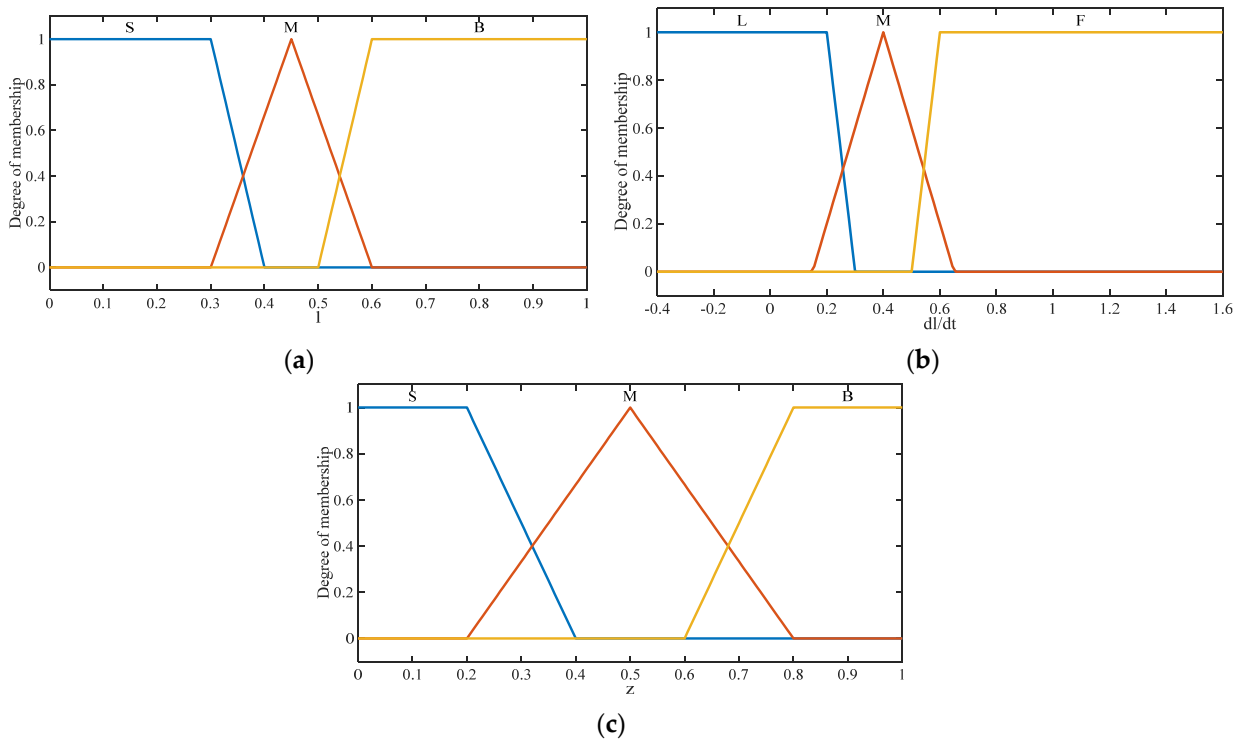

Figure 7. Affiliation function of the fuzzy controller for brake intention recognition. (**a**) Brake pedal opening; (**b**) Brake pedal opening rate of change; (**c**) Brake strength.

For the regenerative braking duty ratio fuzzy controller, the fuzzy domains of the input variables vehicle speed *V* and *SOC* are defined as [0, 140] and [0, 1], and the fuzzy subsets are {S (Small), M (Medium), B (Big)} and {S (Small), M (Medium), B (Big)}, respectively; the fuzzy domain of the regenerative braking duty ratio *K* is defined as [0, 1], and the fuzzy subsets are {VS (Very Small), S (Small), M (Medium), B (Big), VB (Very Big)}.

The fuzzy rules for the regenerative braking duty ratio fuzzy controller can be outlined as follows: (1) as braking strength increases, reduce the regenerative braking duty ratio; (2) when the vehicle speed is low, motor speed is low and the recoverable energy is small, so the regenerative braking duty ratio can be appropriately reduced; when the vehicle speed is high, the primary consideration is the braking safety, and the regenerative braking duty ratio should be reduced; (3) the bigger the *SOC* of the battery, the more it should be

reduced to ensure battery safety. Hence, the fuzzy rules for the regenerative braking ratio fuzzy controller are shown in Table 2.

Table 2. Fuzzy rules of the fuzzy controller for regenerative braking duty ratio.

Number	*Z*	*V*	*SOC*	*K*	Number	*Z*	*V*	*SOC*	*K*
1	S	S	B	S	**15**	M	B	M	M
2	S	M	B	S	**16**	B	S	M	S
3	S	B	B	S	**17**	B	M	M	S
4	M	S	B	S	**18**	B	B	M	VS
5	M	M	B	S	**19**	S	S	S	S
6	M	B	B	S	**20**	S	M	S	VB
7	B	S	B	VS	**21**	S	B	S	B
8	B	M	B	VS	**22**	M	S	S	S
9	B	B	B	VS	**23**	M	M	S	M
10	S	S	M	S	**24**	M	B	S	M
11	S	M	M	B	**25**	B	S	S	S
12	S	B	M	B	**26**	B	M	S	S
13	M	S	M	S	**27**	B	B	S	VS
14	M	M	M	M					

The surface plot of the identification effect of the regenerative braking duty ratio fuzzy controller, obtained from the fuzzy rules formulated in Table 2 above, is shown in Figure 8.

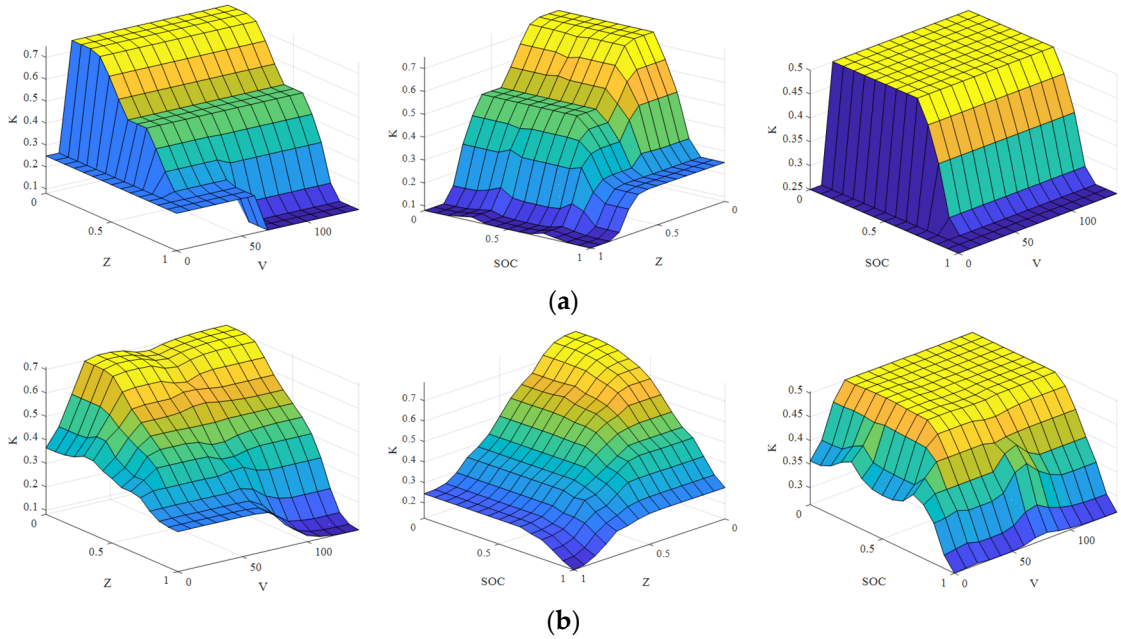

Figure 8. Input and output relationship surface of the fuzzy controller for regenerative braking ratio. (**a**) T_T-type affiliation function; (**b**) G_S-type affiliation function.

Analysis of Figure 8 shows that the regenerative braking duty ratio has the greatest relationship with the strength of braking demand; the greater the strength of braking demand, the smaller the regenerative braking duty ratio. *SOC* and speed play a role in limiting the output regenerative braking duty ratio: when the speed and the *SOC* are too large, there is a certain decline in the output regenerative braking duty ratio. The identification results of the fuzzy controller of regenerative braking duty ratio are in line with the law of braking energy recovery ratio allocation in electric vehicle composite braking systems, which verifies the effectiveness of the fuzzy rules.

The affiliation functions of the input and output variables of the fuzzy controller for regenerative braking duty ratio are shown in Figure 9.

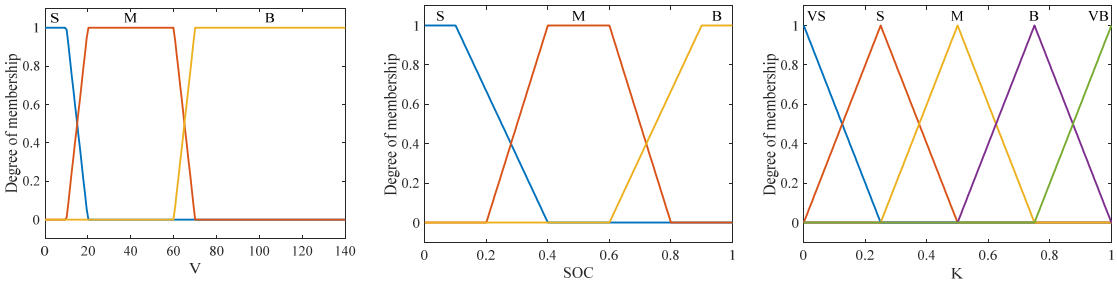

Figure 9. Affiliation function of the fuzzy controller for regenerative braking duty ratio.

3.2.4. Analysis of Controller Results Based on Control Tests

According to the affiliation function in Section 3.2.3, four different dual fuzzy controller models can be designed, which are (1) both dual fuzzy controllers use T_T-type affiliation function; (2) both dual fuzzy controllers use G_S-type affiliation function; (3) braking intention recognition fuzzy controllers use T_T-type affiliation function, and regenerative braking duty ratio fuzzy controllers use G_S-type affiliation function; and (4) the regenerative braking duty ratio fuzzy controller adopts T_T-type affiliation function and the braking intention recognition fuzzy controller adopts G_S-type affiliation function.

In order to choose the optimal dual fuzzy controller for this study, the vehicle speed is set as high-speed, medium-speed, and low-speed (110 km/h, 50 km/h, 25 km/h) for comparison; the braking working conditions are selected as emergency, normal, and slow brake pedal opening with the rate of change {(0.85, 1.2), (0.4, 0.4), (0.2, 0.15)} for comparison. Cross-assigning the vehicle speeds to the braking conditions gives nine braking modes, as shown in Table 3.

Table 3. Parameter table of nine braking modes.

Braking Strength \ Speed	High	Medium	Low
Emergency	(0.85, 1.2, 110)	(0.85, 1.2, 50)	(0.85, 1.2, 25)
Normal	(0.4, 0.4, 110)	(0.4, 0.4, 50)	(0.4, 0.4, 25)
Slow	(0.2, 0.15, 110)	(0.2, 0.15, 50)	(0.2, 0.15, 25)

The regenerative braking percentage data for the nine braking modes are shown in Tables 4–6.

Table 4. Regenerative braking percentage in high-speed braking mode.

Affiliation Function \ Braking Mode	High-Speed Emergency Braking	High-Speed Normal Braking	High-Speed Slow Braking
T_T + T_T	8.00%	50.00%	75.00%
G_S + G_S	20.01%	50.36%	57.13%
T_T + G_S	13.36%	49.70%	64.22%
G_S + T_T	12.87%	50.00%	61.43%

Table 5. Regenerative braking percentage in medium-speed braking mode.

Affiliation Function \ Braking Mode	High-Speed Emergency Braking	High-Speed Normal Braking	High-Speed Slow Braking
T_T + T_T	25.00%	50.00%	75.00%
G_S + G_S	28.38%	50.34%	60.94%
T_T + G_S	26.24%	49.71%	64.59%
G_S + T_T	26.23%	50.00%	67.10%

Table 6. Regenerative braking percentage in low-speed braking mode.

Affiliation Function \ Braking Mode	High-Speed Emergency Braking	High-Speed Normal Braking	High-Speed Slow Braking
T_T + T_T	25.00%	50.00%	75.00%
G_S + G_S	28.38%	50.17%	56.90%
T_T + G_S	26.27%	49.52%	63.98%
G_S + T_T	26.23%	50.00%	61.43%

Considering that the regenerative braking strategy is mainly applied to urban driving scenarios, in such scenarios, the vehicle spends most of its time in normal braking and slow braking states. Therefore, the weights of these two braking modes should be increased. After a comprehensive analysis, 'T_T + T_T' is chosen as the structure of the double fuzzy controller in this paper.

3.3. Modification of Regenerative Braking Control Strategy

As mentioned above, the regenerative braking duty ratio is not only related to braking strength but also to vehicle speed and battery *SOC*. Here, vehicle speed and battery *SOC* correction factors are introduced to correct motor power.

From the transmission characteristics of the transmission system, it can be seen that motor speed and vehicle traveling speed satisfy the following relationship equation:

$$n = \frac{u \cdot i_g \cdot i_0}{0.377r} \tag{12}$$

where u is the vehicle travelling speed (km/h); n is the motor speed (1/min); i_g is the transmission ratio; i_0 is the main reduction gear ratio; r is the wheel radius (m).

When the vehicle speed is low, the inertial energy of the vehicle traveling is less, and energy recovery in this state is not significant. Therefore, a speed impact factor is introduced: when the speed is low (<5 km/h), the motor does not recovery energy; when the speed of the vehicle is 5–8 km/h, the motor engages in composite braking energy recovery with a degree of linear growth; when the speed is greater than 10 km/h, the motor operates normally to carry out composite braking energy recovery, and the correction factor function is:

$$Corr_1 = \begin{cases} 0 & v < 5\text{km/h} \\ 0.2v - 1, & 5\text{km/h} \le v \le 10\text{km/h} \\ 1 & v > 10\text{km/h} \end{cases} \tag{13}$$

where $Corr_1$ is the speed correction factor.

The power battery, being the sole energy provider for the all-electric vehicle, must prioritize safety; thus, a safety threshold should be set at different *SOC* values. When the battery *SOC* value reaches the upper limit of the threshold, the motor does not participate in the regenerative braking process. Therefore, the battery *SOC* influence factor is introduced: when the battery *SOC* value reaches 95%, the motor exits regenerative braking; when the battery *SOC* value reaches 85%, the motor's participation in regenerative braking should be gradually reduced, and its correction factor function is:

$$Corr_2 = \begin{cases} 1 & SOC < 85\% \\ 10(0.95 - SOC), & 85\% \le SOC \le 95\% \\ 0 & SOC > 95\% \end{cases} \tag{14}$$

where $Corr_2$ is the *SOC* correction factor.

To summarize, Figure 10 displays the relationship between vehicle speed, *SOC*, and motor power correction.

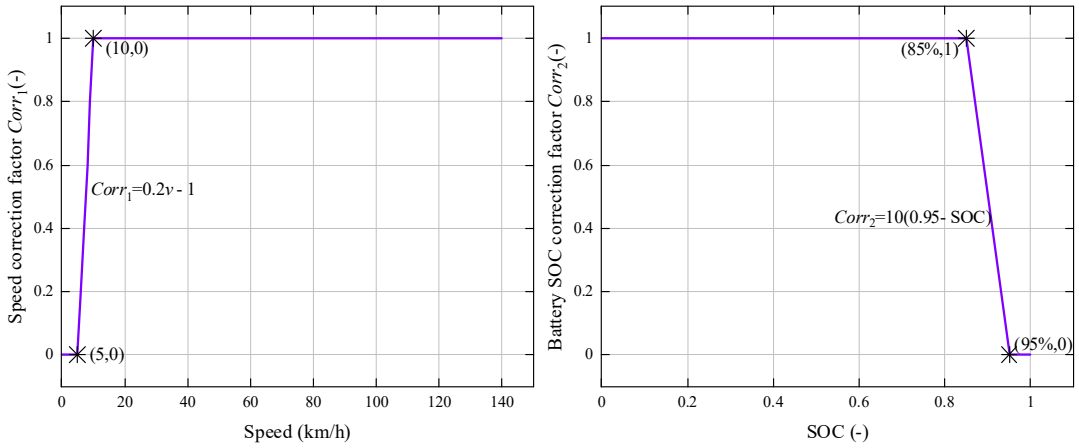

(**a**) (**b**)

Figure 10. Plot of vehicle speed as a function of battery *SOC* correction factor. (**a**) Speed correction factor; (**b**) *SOC* correction factor.

The power value of the motor mechanism, corrected for the two factors of vehicle speed and battery *SOC*, is:

$$F_{mot\_reg\_2} = F_{mot\_reg\_1} \cdot Corr_1 \cdot Corr_2 \quad (15)$$

where $F_{mot\_reg\_2}$ is the corrected actual motor power (N); $F_{mot\_reg\_1}$ is the corrected pre-modified motor power (N) assigned by the double fuzzy controller.

4. Joint Simulation and Analysis of Results

To validate the efficiency of the dual-fuzzy regenerative braking control strategy proposed in this study, the integrated Matlab/Simulink R2019b and CRUISE 2019 platform uses the joint simulation of Dynamic Link Library (DLL) to simulate and evaluate the control strategy using the New European Driving Cycle (NEDC) and Extra Urban Driving Cycle (EUDC). The simulation validation covers feasibility, energy recovery, and battery *SOC* variations.

4.1. Feasibility Simulation

Based on the control strategy of this paper, the vehicle's following characteristics are simulated and tested under NEDC and EUDC conditions, as shown in Figure 11.

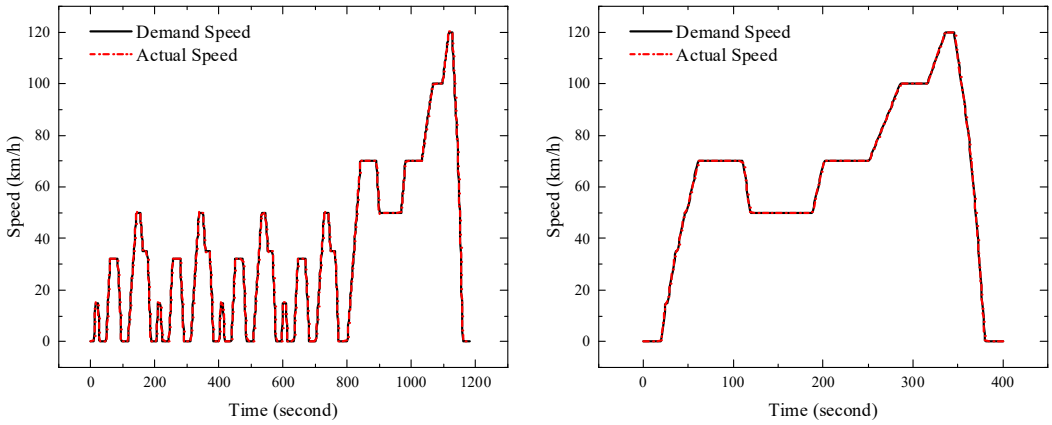

(**a**) (**b**)

Figure 11. Vehicle speed follows under different cycle conditions. (**a**) Speed following under NEDC conditions; (**b**) Speed following under EUDC conditions.

Figure 11 shows the actual vehicle speed of this paper's control strategy under NEDC conditions, and EUDC conditions can follow the demand speed, which verifies the feasibility of the control strategy.

4.2. Energy Recovery Simulation

The control strategy in this paper, a single fuzzy control, and a parallel control strategy were simulated and tested for energy recovery of the vehicle under two cycle conditions. Energy recovery is depicted in Figure 12, while battery *SOC* variation is change in Figure 13.

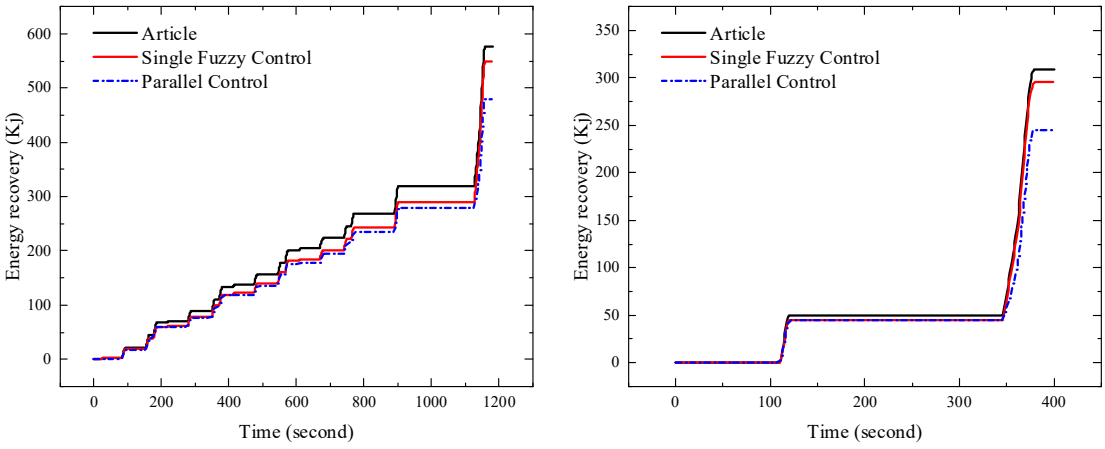

Figure 12. Energy recovery under different cycle conditions. (**a**) Energy recovery under NEDC conditions; (**b**) Energy recovery under EUDC conditions.

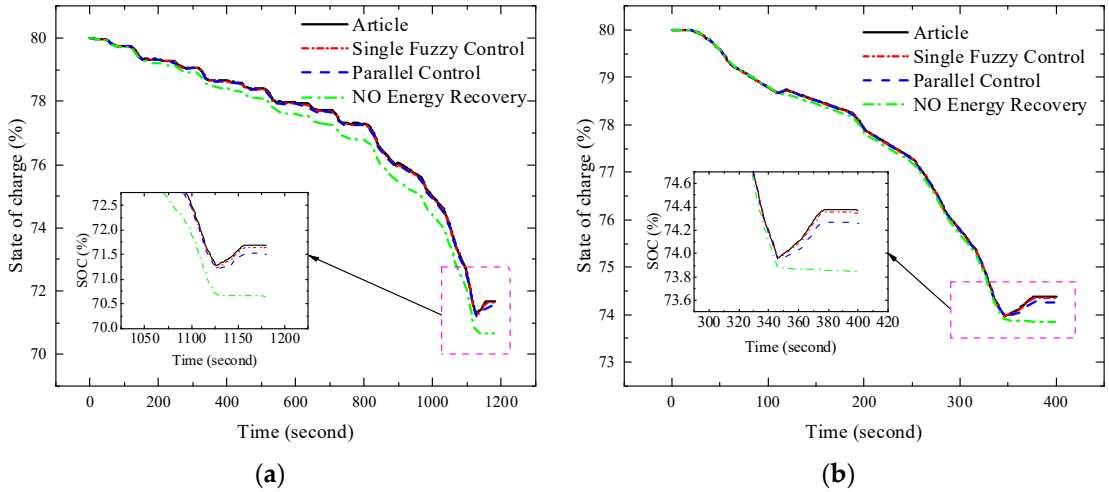

Figure 13. Variation of battery *SOC* under different cycle conditions. (**a**) *SOC* under NEDC conditions; (**b**) *SOC* under EUDC conditions.

From Figure 12, it can be seen that, under the same conditions, the control strategy in this paper can recover more braking energy, which verifies the superiority of the control strategy in energy recovery. The energy recovery is shown in Table 7.

As shown in Table 7, the control strategy in this paper has the largest energy recovery values of 576.29 kJ and 309.36 kJ for both NEDC and EUDC cycles. Compared to a single fuzzy control strategy and a parallel control strategy, the energy recovery can be increased by 26.26 kJ and 96.13 kJ, respectively, for a single NEDC condition.

Table 7. Energy recovery of different control strategies under two cycle conditions.

Cycle Conditions \ Control Strategies	Article	Single Fuzzy Control	Parallel Control
NEDC (kJ)	576.29	550.03	480.16
EUDC (kJ)	309.36	295.27	245.45

Analyzing Figure 13, it can be seen that, under the same conditions, the battery *SOC* under the control strategy of this paper decreases slowly compared with other strategies. This further confirms the energy-efficient characteristics of the proposed control strategy. When the initial *SOC* is 80, the final value of the *SOC* at the end of the simulation is shown in Table 8.

Table 8. Battery *SOC* for different control strategies under two cycle conditions.

Cycle Conditions \ Control Strategies	Article	Single Fuzzy Control	Parallel Control	No Energy Recovery
NEDC (%)	71.68	71.63	71.51	70.65
EUDC (%)	74.37	74.34	74.26	73.84

Data analysis from Table 8 indicates a higher final battery *SOC* value with the control strategy presented, which increases by 0.05%, 0.17%, and 1.03%, respectively, compared to the single fuzzy control, parallel control strategy, and the strategy with no energy recovery under NEDC operating conditions.

5. Conclusions

A dual-fuzzy regenerative braking control strategy based on braking intention recognition is proposed for the electromechanical composite braking system of pure electric vehicles. The designed dual-fuzzy logic controller includes a braking intention recognition fuzzy controller and a regenerative braking ratio fuzzy controller. Different controller structures affect the regenerative braking ratio; a control test is set up to compare and analyze four different dual-fuzzy controller models, and the structure of the dual-fuzzy controller is finally determined by comprehensively considering energy recovery and driving scenarios. In addition, two correction factors, vehicle speed and battery *SOC*, are introduced to correct the power of the motor for the effects of low-speed and high-*SOC* states on the motor. Finally, the energy recovery effects of this paper's control strategy, single fuzzy control, and parallel control are compared by Matlab/Simulink R2019b and CRUISE 2019 joint simulation.

The simulation results show that the dual fuzzy regenerative braking control strategy has better energy recovery than the single fuzzy parallel control strategy, which can recover 576.29 kJ and 309.36 kJ of energy under NEDC and EUDC cycling conditions, respectively; the battery *SOC* decreases more slowly under the same conditions. Under single NEDC and EUDC operating conditions, the control strategy can improve the energy recovery by 26.26 kJ, 96.13 kJ and 14.09 kJ, 63.91 kJ, respectively.

From this study, it can be found that the factors affecting braking energy recovery include not only vehicle speed, *SOC*, and braking strength, but also the structure of the fuzzy controller used for braking intention recognition and power optimisation of the motor mechanism.

Author Contributions: Methodology, Z.Z.; software, Y.Q.; formal analysis, J.C.; resources, Z.Z.; data curation, J.C.; writing—original draft preparation, Y.Q.; writing—review and editing, Z.Z.; project administration, Y.Q.; funding acquisition, Z.Z. All authors have read and agreed to the published version of the manuscript.

Funding: This research was funded by the National Natural Science Foundation of China (51875494), the Natural Science Research Program of Jiangsu Province Colleges and Universities (19KJB580019), the Jiangsu Normal University Graduate Innovation Program Project (SJCX20_1353), and the Graduate innovation program of Yancheng institute of technology (SJCX23_XY052).

Data Availability Statement: The data that support the findings of this study are available from the corresponding author upon reasonable request.

Conflicts of Interest: The authors declare no conflicts of interest.

References

1. He, X.; Liu, H.; He, S.; Hu, B.; Xiao, G. Research on the energy efficiency of energy regeneration systems for a battery-powered hydrostatic vehicle. *Energy* **2019**, *178*, 400–418. [CrossRef]
2. Liu, H.; Lei, Y.; Fu, Y.; Li, X. Multi-Objective Optimization Study of Regenerative Braking Control Strategy for Range-Extended Electric Vehicle. *Appl. Sci.* **2020**, *10*, 1789. [CrossRef]
3. Zhao, D.; Chu, L.; Xu, N.; Sun, C.; Xu, Y. Development of a Cooperative Braking System for Front-Wheel Drive Electric Vehicles. *Energies* **2018**, *11*, 378. [CrossRef]
4. Li, W.; Du, H.; Li, W. Driver intention based coordinate control of regenerative and plugging braking for electric vehicles with in-wheel PMSMs. *IET Intell. Transp. Syst.* **2018**, *12*, 1300–1311. [CrossRef]
5. Xu, W.; Chen, H.; Wang, J.; Zhao, H. Velocity Optimization for Braking Energy Management of In-Wheel Motor Electric Vehicles. *IEEE Access* **2019**, *7*, 66410–66422. [CrossRef]
6. Vellenga, K.; Steinhauer, H.J.; Karlsson, A. Driver intention recognition: State-of-the-art review. *IEEE Open J. Intell. Transp. Syst.* **2022**, *3*, 602–616. [CrossRef]
7. Wen, J.; Zhang, H.; Li, Z.; Fang, X. Research on Electric Vehicle Braking Intention Recognition Based on Sample Entropy and Probabilistic Neural Network. *World Electr. Veh. J.* **2023**, *14*, 264. [CrossRef]
8. Hernandez, L.; Martinez, E.; Antelis, J. Detection of Emergency Braking Intention Using Driver's Electroencephalographic Signals. *IEEE Lat. Am. Trans.* **2019**, *17*, 111–118. [CrossRef]
9. Li, M.; Wang, W.; Liu, Z.; Qiu, M.; Qu, D. Driver Behavior and Intention Recognition Based on Wavelet Denoising and Bayesian Theory. *Sustainability* **2022**, *14*, 6901. [CrossRef]
10. Haufe, S.; Kim, J.W.; Kim, I.H.; Sonnleitner, A.; Schrauf, M.; Curio, G.; Blankertz, B. Electrophysiology-based detection of emergency braking intention in real-world driving. *J. Neural Eng.* **2014**, *11*, 056011. [CrossRef]
11. Mora, H.J.; Pino, E.J. Simplified Prediction Method for Detecting the Emergency Braking Intention Using EEG and a CNN Trained with a 2D Matrices Tensor Arrangement. *Int. J. Hum.–Comput. Interact.* **2022**, *39*, 587–600. [CrossRef]
12. Hernández, L.G.; Mozos, O.M.; Ferrández, J.M.; Antelis, J.M. EEG-based detection of braking intention under different car driving conditions. *Front. Neurosci.* **2018**, *12*, 29. [CrossRef] [PubMed]
13. Tang, J.; Zuo, Y.Y. Braking Intention Recognition Method Based on the Fuzzy Neural Network. *Wirel. Commun. Mob. Comput.* **2022**, *2022*, 2503311. [CrossRef]
14. Jia, Q.; Tang, P. Simulation of Electric Vehicle Regenerative Braking Control Strategy Based on Brake Intention Recognition. *J. Phys. Conf. Ser.* **2023**, *2492*, 012018. [CrossRef]
15. Yang, W.; Liu, J.; Zhou, K.; Zhang, Z.; Qu, X. An Automatic Emergency Braking Model considering Driver's Intention Recognition of the Front Vehicle. *J. Adv. Transp.* **2020**, *2020*, 5172305. [CrossRef]
16. Wang, S.; Zhao, X.; Yu, Q.; Yuan, T. Identification of driver braking intention based on long short-term memory (LSTM) net-work. *IEEE Access* **2020**, *8*, 180422–180432. [CrossRef]
17. Jiang, B.; Zhang, X.W.; Wang, Y.X. Regenerative Braking Control Strategy of Electric Vehicles Based on Braking Stability Requirements. *Int. J. Automot. Technol.* **2021**, *22*, 465–473.
18. Liu, F. A PMSM fuzzy logic regenerative braking control strategy for electric vehicles. *J. Intell. Fuzzy Syst.* **2021**, *41*, 4873–4881. [CrossRef]
19. Pei, X.; Pan, H.; Chen, Z.; Guo, X.; Yang, B. Coordinated control strategy of electro-hydraulic braking for energy regeneration. *Control. Eng. Pract.* **2020**, *96*, 104324. [CrossRef]
20. He, Q.; Yang, Y.; Luo, C.; Zhai, J.; Luo, R.; Fu, C. Energy recovery strategy optimization of dual-motor drive electric vehicle based on braking safety and efficient recovery. *Energy* **2022**, *248*, 123543. [CrossRef]
21. Zhang, J.; Yang, Y.; Qin, D.; Fu, C.; Cong, Z. Regenerative Braking Control Method Based on Predictive Optimization for Four-Wheel Drive Pure Electric Vehicle. *IEEE Access* **2021**, *9*, 1394–1406. [CrossRef]
22. Zhang, Y.; Wang, W.; Xiang, C.; Yang, C.; Peng, H.; Wei, C. A swarm intelligence-based predictive regenerative braking control strategy for hybrid electric vehicle. *Veh. Syst. Dyn.* **2022**, *60*, 973–997. [CrossRef]
23. Geng, C.; Ning, D.; Guo, L.; Xue, Q.; Mei, S. Simulation Research on Regenerative Braking Control Strategy of Hybrid Electric Vehicle. *Energies* **2021**, *14*, 2202. [CrossRef]

24. Li, X.; Ma, J.; Zhao, X.; Wang, L. Study on Braking Energy Recovery Control Strategy for Four-Axle Battery Electric Heavy-Duty Trucks. *Int. J. Energy Res.* **2023**, *2023*, 1868528. [CrossRef]
25. Liang, C.; Zheng, Z.A. Research on composite braking control strategy of battery electric vehicle based on road surface recognition. *Proc. Inst. Mech. Eng. Part D J. Automob. Eng.* **2024**, *238*, 788–801. [CrossRef]